



Cite this: *Dalton Trans.*, 2018, **47**, 14184

Received 20th April 2018,

Accepted 15th June 2018

DOI: 10.1039/c8dt01580e

rsc.li/dalton

## Solid-state sensors based on Eu<sup>3+</sup>-containing supramolecular polymers with luminescence colour switching capability†

L. N. Neumann, <sup>a</sup> C. Calvino, <sup>a</sup> Y. C. Simon, <sup>a,b</sup> S. Schrettl <sup>a</sup> and C. Weder <sup>\*a</sup>

**Polymers that exhibit changes of their luminescence colour in response to external stimuli are attractive candidates for sensing systems. We herein report the preparation of europium-based metallosupramolecular polymers, which can be processed into films and coatings that display readily detectable luminescence colour changes in response to various types of analytes.**

Metal–ligand complexes of selected lanthanide cations display a strong luminescence in the visible range, rendering them ideal sensors for the detection of various chemicals,<sup>1,2</sup> including chemical warfare agents (CWAs).<sup>3,4</sup> The response is typically caused by a modulation of the metal-centred emission in presence of the analyte. A luminescence turn-on can be achieved by designing systems in which the analyte displaces a quenching group from the lanthanide coordination sphere. Alternatively, a luminescence turn-off is possible when the analyte causes the displacement of the sensitizing antenna or alteration of its photophysical properties.<sup>5</sup> For example, the emission of lanthanide-terpyridine complexes is quenched upon exposure to G-type CWAs,<sup>6</sup> and changes of the complex luminescence of a 2,6-bis(1'-methylbenzimidazolyl)pyridine (Mebip) ligand with different lanthanide ions have been exploited to selectively detect various aliphatic organophosphates.<sup>7</sup>

A visually detectable change of the luminescence colour (as opposed to a turn-on or turn-off effect) can enable an improved readout, potentially furnish a ratiometric response,<sup>8–10</sup> and is especially useful when spectroscopic equipment is not available.<sup>11,12</sup> However, only few examples of lanthanide-based sensor complexes that display such a colour switch are known.<sup>2</sup> For instance, an Ir(III)/Eu(III) dyad was shown to change the

luminescence colour upon exposure to the V-series CWA mimic 2-diisopropylaminoethyl ethyl methylphosphonate (VO) by selectively quenching the red Eu-based emission.<sup>13</sup> In another report, norbornene-derived terpyridine monomers complexed to Eu(III) exhibited a magenta-to-blue colour change upon exposure to G-type CWAs.<sup>14</sup> These low-molecular weight solvent-based sensory systems demonstrate the potential benefits of luminescence colour changes, and similar responses were also achieved with metallosupramolecular polymer (MSP) networks that feature combinations of transition or lanthanide metal ions due to a selective quenching of some of the metal-based emission.<sup>15,16</sup> A direct monitoring of the disassembly with a potential increase in sensitivity may be achieved by employing ligands that feature a distinct emission in the visible range, which has, to the best of our knowledge, not been explored in polymeric solid-state materials so far.

We herein report a lanthanide-based MSP system that features a distinct and clearly visible emission colour change due to the vastly different emission characteristics of the metal–ligand complex, and the telechelic, ligand-carrying macromonomer. Red-light emitting MSP films are obtained upon assembling the macromonomer with europium perchlorate and a clearly visible luminescence colour change is observed in response to different stimuli such as heat, exposure to solvents, or other analytes that disrupt or alter the metal–ligand complexes. The distinct colour change constitutes a visually detectable signal that indicates exposure to the various analytes and may allow for an *in situ* optical monitoring.

The basis of the approach used in our study are tridentate Mebip ligands, which are known to act as efficient “antennas” for lanthanide ions.<sup>17</sup> However, Mebip itself does not fluoresce in the visible range. To shift the fluorescence of this motif into the visible range, an extension of the conjugated  $\pi$ -system was pursued. Thus, 2,6-bis(1'-methylbenzimidazolyl)-4-bromopyridine was prepared following literature procedures and its coupling to 4-ethynylaniline under Sonogashira conditions yielded the desired  $\pi$ -extended Mebip derivative (Fig. S1†).<sup>18,19</sup> Subsequently, this ligand was coupled to dodecanoic acid and bis-carboxylic acid functionalised telechelic poly(ethylene-co-

<sup>a</sup>Adolphe Merkle Institute, University of Fribourg, Chemin des Verdiers 4, CH-1700 Fribourg, Switzerland. E-mail: christoph.weder@unifr.ch

<sup>b</sup>School of Polymer Science and Engineering, The University of Southern Mississippi, 118 College Dr., Box 5050, Hattiesburg, Mississippi, 39406, USA

†Electronic supplementary information (ESI) available: A comprehensive account of all experimental details, including synthetic procedures, analytical data, and NMR spectra of all novel compounds is provided. See DOI: 10.1039/c8dt01580e



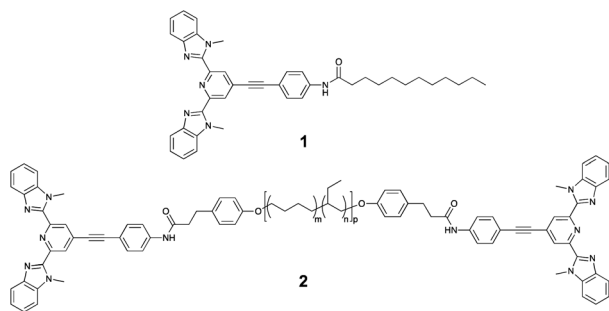


**Fig. 1** Chemical structure of the low-molecular weight reference ligand **1** and the telechelic poly(ethylene-co-butylene) (PEB) macromonomer **2** (with  $M_n = 4200 \text{ g mol}^{-1}$ ;  $m \approx 0.36$ ,  $n \approx 0.64$ ,  $p \approx 55$ ).

butylene) *via* carbodiimide-mediated esterification reactions to furnish a low-molecular weight reference ligand **1** and the macromonomer **2**, respectively (Fig. 1).

To demonstrate that the extended ligand forms complexes in the same manner as the parent Mebip derivatives, solutions of **1** ( $c = 20 \mu\text{mol L}^{-1}$ ) and **2** ( $c = 9 \mu\text{mol L}^{-1}$ ) in  $\text{CHCl}_3/\text{MeCN}$  (9 : 1) were titrated with  $\text{Zn}(\text{NTf}_2)_2$ , which binds more strongly to Mebip derivatives than lanthanides.<sup>17</sup> UV-Vis spectroscopy was used to follow the formation of the coordination complexes with a 1 : 2 metal : ligand stoichiometry (Fig. 2a and b). For both compounds, the absorption band of the ligand at 332 nm shifted to 388 nm and the series of spectra display an isosbestic point at 359 nm. Plots of the intensity of the characteristic ligand-to-metal charge-transfer band at 388 nm against the  $\text{Zn}^{2+}$ -to-ligand ratio confirmed the conversion to the 1 : 2 coordination complex at a 1 : 2 metal-to-ligand ratio (denoted as **1:Zn** in the following, Fig. S2 and S3†). Thus, the absorption spectra corroborate that the  $\pi$ -extended ligand derivative **1** and the macromonomer **2** coordinate metal-ions in the same way as the parent Mebip derivative.<sup>17,19,20</sup>

Similarly, solutions of **1** ( $c = 20 \mu\text{mol L}^{-1}$ ) and **2** ( $c = 10 \mu\text{mol L}^{-1}$ ) in a  $\text{CHCl}_3/\text{MeCN}$  mixture (9 : 1) were titrated with  $\text{Eu}(\text{ClO}_4)_3$  and the complex formation was again monitored by UV-Vis spectroscopy. The acquired spectra reveal that the band associated with the ligand absorption at 332 nm shows a more moderate decrease upon addition of  $\text{Eu}^{3+}$  ions than the corresponding titration with  $\text{Zn}(\text{NTf}_2)_2$  and instead of a peak at 388 nm, a broad shoulder centred at 362 nm appears (Fig. 2c, d and S4, S5†). The spectra continue to change if the metal : ligand ratio is increased beyond 1 : 3, and even when the addition of  $\text{Eu}(\text{ClO}_4)_3$  caused no further changes, no ligand-to-metal charge-transfer band became apparent. Similar results were also obtained when the same titration of **1** was carried out at a 10-times higher concentration ( $c = 240 \mu\text{mol L}^{-1}$ , Fig. S5†). However, when a solution of **1** was titrated with  $\text{Eu}(\text{ClO}_4)_3$  in MeCN ( $c = 21 \mu\text{mol L}^{-1}$ ), a distinct band at 388 nm appeared at a metal : ligand ratio of 1 : 3, indicating the formation of the metal-ligand complex (Fig. 2e). The spectra continue to change upon addition of more  $\text{Eu}(\text{ClO}_4)_3$  and level off at a metal : ligand ration of approximately 1 : 1, as observed from plots of the intensity of the

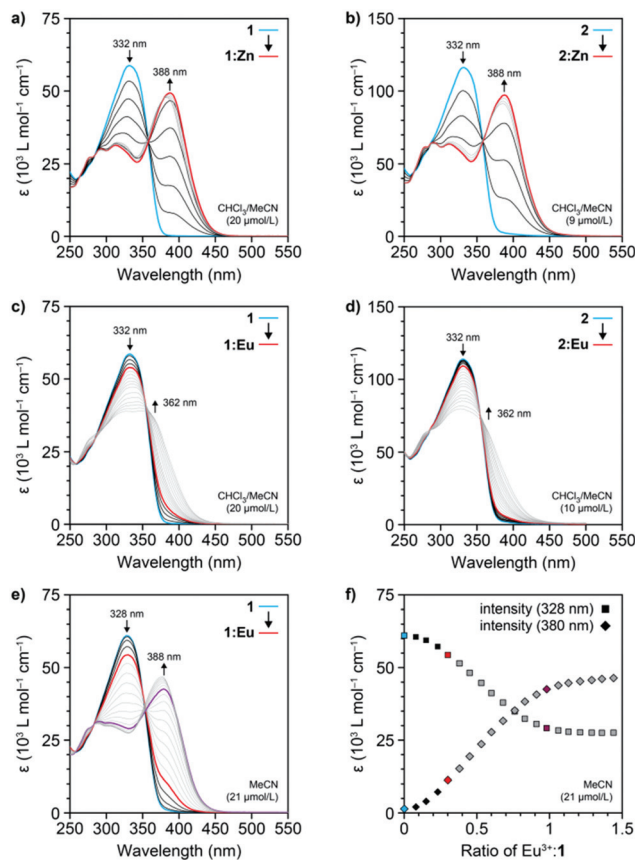


**Fig. 2** UV-Vis absorption spectra of solutions of (a) ligand **1** ( $c = 20 \mu\text{mol L}^{-1}$  in  $\text{CHCl}_3/\text{MeCN}$  9 : 1, blue line) and (b) macromonomer **2** ( $c = 9 \mu\text{mol L}^{-1}$  in  $\text{CHCl}_3/\text{MeCN}$  9 : 1, blue line). Upon titration with aliquots of  $\text{Zn}(\text{NTf}_2)_2$ , the formation of the coordination complexes is observed at metal-to-ligand ratios of 1 : 2 (red lines). (c, d) UV-Vis absorption spectra of solutions of (c) ligand **1** ( $c = 20 \mu\text{mol L}^{-1}$  in  $\text{CHCl}_3/\text{MeCN}$  9 : 1, blue line) and (d) macromonomer **2** ( $c = 10 \mu\text{mol L}^{-1}$  in  $\text{CHCl}_3/\text{MeCN}$  9 : 1, blue line) and spectra upon titration with aliquots of  $\text{Eu}(\text{ClO}_4)_3$  (red lines highlight the 1 : 3 metal-to-ligand ratios). (e) UV-Vis absorption spectra of **1** ( $c = 21 \mu\text{mol L}^{-1}$  in MeCN, blue line). Upon titration with aliquots of  $\text{Eu}(\text{ClO}_4)_3$  a distinct band at 388 nm appears, indicating the formation of the complex at a 1 : 3 metal : ligand ratio (red line). (f) Plots of the absorption intensities of **1** (328 nm) and the 1 :  $\text{Eu}^{3+}$  complex (388 nm) against the europium-salt-to-ligand ratio show a levelling off at the stoichiometric 1 : 1 ratio.

characteristic ligand and complex absorptions at 328 and 388 nm, respectively (Fig. 2f). When the same titration of **1** was carried out at a 10-fold higher concentration ( $c = 208 \mu\text{mol L}^{-1}$ ), the dynamic equilibrium of the complex formation was shifted and the levelling off was already observed at a 1 : 1.5 metal : ligand ratio (Fig. S6†). Hence, due to the lower binding constant of the  $\text{Eu}^{3+}$  coordination complex *vis-à-vis* the  $\text{Zn}^{2+}$  complex, notably in  $\text{CHCl}_3$ ,<sup>17</sup> unbound ligand remains present in dilute solutions of **1** and **2** at a stoichiometric 1 : 3 metal-to-ligand ratio. Indeed, the spectrophotometric titrations in MeCN follow the previously reported behaviour of the parent Mebip ligand,<sup>17</sup> corroborating the successive formation of the 1 : 3, 1 : 2, and 1 : 1 complexes between the  $\text{Eu}^{3+}$ -ions and **1**.



As a result of the extended conjugation system in the Mebip ligand used here, solutions of **1** and **2** show a bright blue fluorescence under UV light illumination ( $\lambda_{\text{ex}} = 365$  nm) that is clearly visible to the unassisted eye (Fig. 3 and S7†). The fluorescence spectra of **1** ( $c = 21 \mu\text{mol L}^{-1}$  in MeCN) and **2** ( $c = 10 \mu\text{mol L}^{-1}$  in  $\text{CHCl}_3/\text{MeCN}$  9:1) display broad emission bands with maxima at 412 and 397 nm, respectively (Fig. 3a and S7, S8†). Spectra obtained upon titration of a solution of **2** ( $c = 10 \mu\text{mol L}^{-1}$ ) with  $\text{Zn}(\text{NTf})_2$  show a significant drop of the intensity of the ligand emission at 397 nm and a concomitant development of a broad band at 520 nm, associated with the  $\text{Zn}^{2+}$ -complex (Fig. S8†). In accordance with the absorption spectra, plots of the free ligand emission intensity against the zinc-salt-to-ligand ratio show that the latter disappears completely when a 1:2 metal-to-ligand ratio is reached. Spectrophotometric titrations of **2** ( $c = 10 \mu\text{mol L}^{-1}$ ) with  $\text{Eu}(\text{ClO}_4)_3$  show a similar decrease of the intensity of the ligand band together with a sharp increase of the  $\text{Eu}^{3+}$ -based  $^5\text{D}_0 \rightarrow ^7\text{F}_j$  transitions, of which the  $^5\text{D}_0 \rightarrow ^7\text{F}_2$  transition ( $\lambda_{\text{max}} = 618$  nm) is the most intense (Fig. 3a). As expected on the basis of the absorption spectra, solutions with a 1:3 metal-to-ligand ratio exhibit emission from the metal-ligand complex as well as emission from the free ligand on account of the incomplete

complexation in  $\text{CHCl}_3/\text{MeCN}$ ; such solutions display a magenta-coloured emission (Fig. 3b). When similar titrations with  $\text{Eu}(\text{ClO}_4)_3$  were carried out with the reference ligand **1** in MeCN solutions ( $c = 21 \mu\text{mol L}^{-1}$ ), the maximum emission intensity of the  $\text{Eu}^{3+}$ -based  $^5\text{D}_0 \rightarrow ^7\text{F}_2$  transition at 618 nm was reached at a 1:3 metal-to-ligand ratio, indicating the formation of the 1:3 coordination complex (denoted as **2:Eu** in the following, Fig. S7†). In contrast to the titrations with  $\text{Zn}^{2+}$ , residual ligand emission is observed at this 1:3 ratio, which can be explained on the basis of the lower binding constant and the dynamic nature of the  $\text{Eu}^{3+}$ -complexes. In addition, excitation spectra of the ligand **1** and macromonomer **2** (Fig. S9†), as well as their corresponding  $\text{Zn}^{2+}$ - and  $\text{Eu}^{3+}$ -complexes were recorded in order to probe for the origin of the observed luminescence (Fig. S10†). Indeed, the spectra indicate that the emission of the complexes originates from the antenna effect of the ligand rather than a possible direct sensitization.<sup>21</sup>

The dynamic equilibrium of the complexes that is present in solution shifts completely to the bound state when the solvent is removed. To achieve a slow evaporation rate and allow the MSP to assemble, chlorobenzene/MeCN solutions (9:1) of **2** ( $c = 164 \mu\text{mol L}^{-1}$ ) were used throughout. The latter show the same spectroscopic behaviour in titrations with  $\text{Eu}(\text{ClO}_4)_3$  (Fig. S11†), and when the corresponding solutions with increasing metal-to-ligand ratios between 0:3 and 1:3 were drop-cast onto glass slides, the luminescence colour was shifted to  $\text{Eu}^{3+}$ -based emission (Fig. 3c). Indeed, in stark contrast to the observations in solution, the thin, drop-cast films with a 1:3 metal-to-ligand ratio for the  $\text{Eu}^{3+}$ -based MSP (**2:Eu**) show a strong, red emission. A comparison of the corresponding solid-state fluorescence spectra of films of macromonomer **2** and the MSP **2:Eu** films prepared from chlorobenzene/MeCN solutions ( $c = 164 \mu\text{mol L}^{-1}$ ) confirms these visual observations (Fig. 3d). Thus, the spectrum of **2** shows a broad emission maximum at 505 nm, revealing a significant red-shift *vis-à-vis* the solution. The spectrum of **2:Eu** shows prominent  $\text{Eu}^{3+}$ -based emission bands, of which the most intense is associated with the  $^5\text{D}_0 \rightarrow ^7\text{F}_2$  transition and seen at 617 nm; the emission of the ligand is almost completely suppressed. Moreover, when spectra of the solid samples of macromonomer **2** and the MSP **2:Eu** films were recorded with different excitation wavelengths ( $\lambda_{\text{ex}} = 340, 355, 370, 374$  nm), the same emission behaviour with only minor changes to the relative emission intensities were observed, corroborating that energy transfer leads to the observed luminescence (Fig. S12a and b†).

As a first experiment related to probing the reversible switching of the luminescence colour of MSP **2:Eu** upon dis- and reassembly, the emission properties of solutions and solid films were investigated as a function of temperature. Thus, step-wise heating of a  $\text{CHCl}_3/\text{MeCN}$  (9:1) solution with a 1:3 metal-to-ligand ratio (**2:Eu**,  $c = 2.5 \mu\text{mol L}^{-1}$ ) to temperatures of 50 °C led to a decrease of the intensity of the red,  $\text{Eu}^{3+}$ -based  $^5\text{D}_0 \rightarrow ^7\text{F}_2$  emission at 617 nm (Fig. 3e, f and S13†). In parallel a readily discernible change of the luminescence colour from magenta to blue could be observed. Upon cooling, the original spectra and colour were recovered, consistent with

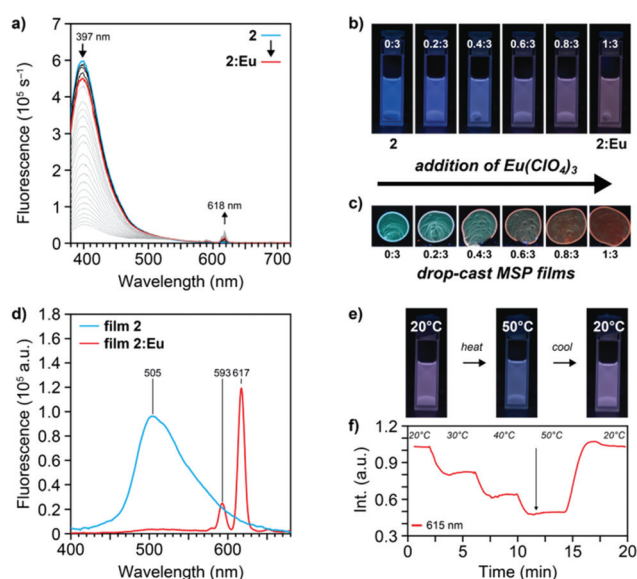


**Fig. 3** (a) Fluorescence spectra of a solution of macromonomer **2** ( $\lambda_{\text{ex}} = 355$  nm,  $c = 10 \mu\text{mol L}^{-1}$  in  $\text{CHCl}_3/\text{MeCN}$  9:1, blue line) upon titration with aliquots of  $\text{Eu}(\text{ClO}_4)_3$ . Free ligand emission persists at a stoichiometric metal-to-ligand ratio of 1:3 (red line). (b) Photographs of solutions of **2** and mixtures of **2** and  $\text{Eu}(\text{ClO}_4)_3$  (metal:ligand ratios as indicated,  $c = 10 \mu\text{mol L}^{-1}$  in  $\text{CHCl}_3/\text{MeCN}$  9:1). (c) Photographs of drop-cast films of **2** and mixtures of **2** and  $\text{Eu}(\text{ClO}_4)_3$  obtained from chlorobenzene/MeCN solutions ( $c = 164 \mu\text{mol L}^{-1}$ ; metal:ligand ratios as indicated). (d) Fluorescence spectra ( $\lambda_{\text{ex}} = 370$  nm) of solid films of **2** and a film **2:Eu** with a 1:3 metal:ligand ratio. (e) Photographs of solutions of **2:Eu** ( $c = 2.5 \mu\text{mol L}^{-1}$  in  $\text{CHCl}_3/\text{MeCN}$  9:1) at room temperature and 50 °C. (f) Emission intensity at 615 nm (associated with the metal-ligand complex) recorded upon heating and cooling the solution used in (e). (Images were taken under illumination with 365 nm UV light).





a fully reversible shift of the equilibrium of the MSP to the disassembled state at elevated temperatures.<sup>22</sup> Drop-cast **2:Eu** MSP films were heated to 160 °C to monitor by means of fluorescence spectroscopy to what extent thermally induced disassembly occurs in the solid-state, but only a reversible decrease of the overall luminescence was observed, presumably due to a thermal depopulation of the excited state at elevated temperatures (Fig. S14†). This behaviour bodes well for the use of solid **2:Eu** in chemosensory applications where temperature-independent emission characteristics are desirable.<sup>11</sup>

To determine the chemosensing capabilities of **2:Eu** in the solid state, the optical changes of thin solid films in response to various analytes were explored. Thus, thin films of the MSP **2:Eu** on glass substrates were exposed to DMSO, which is known to act as competitive ligand for Mebip-lanthanide complexes.<sup>23</sup> Direct exposure of a **2:Eu** film to a drop of neat DMSO resulted in an instant luminescence colour change from red to blue/green, suggesting a largely complete disruption of the complexes under these conditions (Fig. 4a). These observations were confirmed by the corresponding solid-state fluorescence spectra, which showed the complete disappearance of the emission of the  $\text{Eu}^{3+}$ -complex luminescence signature at 617 nm upon exposure to DMSO and the appearance of the solid-state emission band of the ligand at 505 nm. The response was found to be completely reversible: upon washing of the films with methanol, the original properties were restored, and the cycle could be repeated without noticeable hysteresis (Fig. 4a). When films of **2:Eu** were placed on top of a vial filled with DMSO kept at room temperature, the emanating vapours were found to be sufficient to trigger the same visual colour change within six minutes (Fig. 4b and S15†), indicating a high sensitivity of such MSP-based sensors.

Films of **2:Eu** were further exposed to several other analytes and the optical responses were monitored qualitatively and/or quantitatively. In one series of experiments, the **2:Eu** films were tested for their capability to detect triethyl phosphate (TEP) as a mimic for phosphate-based CWAs.<sup>3,7</sup> Exposure of the MSP films on glass slides to the vapours emanating from vials containing neat TEP at room temperature indeed led to a loss of the red-coloured emission and a concomitant increase of a blue, ligand-based fluorescence (Fig. 4c), indicating a competitive binding of TEP to the  $\text{Eu}^{3+}$ -ion and ligand displacement.<sup>7</sup> The latter was found to be completely reversible, as the original red emission was recovered when films were left to stand under ambient conditions for 30 min (Fig. 4d). The response time to TEP vapours appears to be associated to its relatively low vapour pressure at room temperature, and direct exposure to a drop of neat TEP furnishes an immediate luminescence colour change. Moreover, the MSP-based sensor was found to be versatile in detecting a range of vapours of different chemical nature. Thus, exposure of **2:Eu** films to the vapours emanating from acids such as trifluoroacetic acid as well as hydrochloric acid (36%) was found to induce a red-to-green colour change of the emission colour within 20 s and corresponding changes of the solid-state fluorescence spectra (Fig. 4e and S16†). In addition to these strong acids, exposure

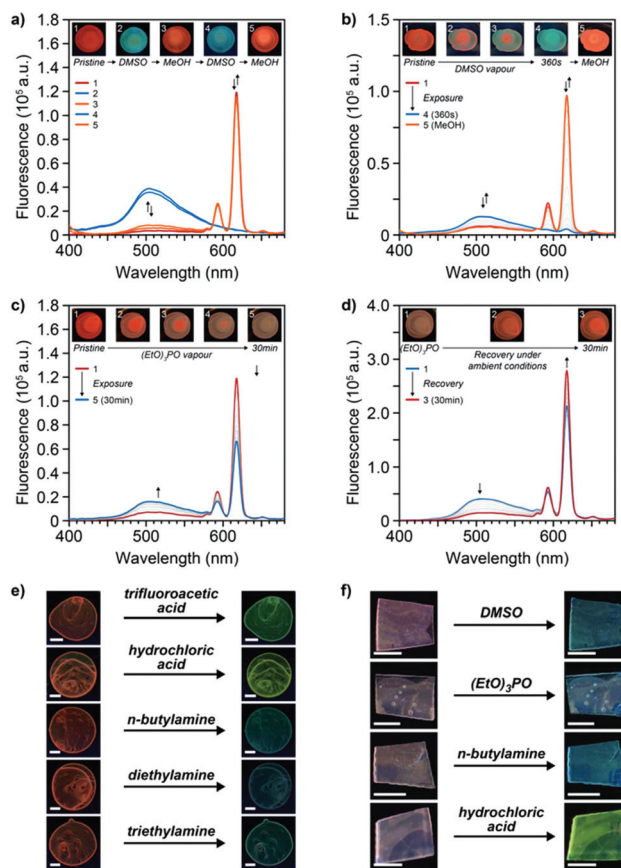


**Fig. 4** Fluorescence spectra ( $\lambda_{\text{ex}} = 370$  nm) and pictures (all taken under illumination with 365 nm UV light) of drop-cast films of the MSP **2:Eu** upon exposure to different analytes. (a) **2:Eu** in its pristine state (1) and upon consecutive exposure to a drop of DMSO (2,4) and washing with MeOH (3,5). (b) **2:Eu** in its pristine state (1) and upon exposure to DMSO vapours (2–4) for up to 360 s, followed by washing with MeOH (5) (spectra normalized at 617 nm). (c) **2:Eu** in its pristine state (1) and upon exposure to  $(\text{EtO})_3\text{PO}$  vapour for up to 30 min (5). (d) Recovery of the sample shown in (c) under ambient conditions. (e) **2:Eu** in its pristine state (left) and upon exposure to trifluoroacetic acid, hydrochloric acid, *n*-butylamine, diethylamine, as well as triethylamine (right). (f) **2:Eu** on an ethylene vinyl alcohol copolymer support in its pristine state (left) and upon exposure to DMSO,  $(\text{EtO})_3\text{PO}$ , *n*-butylamine, and hydrochloric acid (right) (scale bar = 2 mm).

of **2:Eu** films to the vapours of amines was also observed to suppress the red  $\text{Eu}^{3+}$ -based luminescence of the MSPs (Fig. 4e and S16†). Thus, in the presence of vapours of *n*-butylamine, diethylamine, as well as triethylamine a switch to a blue/green, ligand-based fluorescence colour was observed. After exposure to the vapours of amine bases or strong acids, the original luminescence was only partially recovered when films were left to stand under ambient conditions (Fig. S16†), presumably due to a strong coordination of such analytes to the ligand and metal, respectively. To elucidate the nature of the sensing mechanism, titrations of the 1 : 1 coordination complex of **1** and  $\text{Eu}^{3+}$  in MeCN were carried out and UV-Vis spectroscopy was used to follow the changes upon addition of the analytes (Fig. S17–S19†). Thus, the absorption of the unbound ligand



appeared upon addition of DMSO, TEP, and butylamine, indicating a competitive binding of the analyte to the  $\text{Eu}^{3+}$ -metal ion in these cases. By contrast, addition of TFA was found to be accompanied by fundamental changes of the absorption spectra, presumably due to a protonation of the ligand by strong acids that also quenches the emission.

Finally, the potential use of the MSPs as coating on a polymer substrate and their capability for the sensing of the different types of analytes was tested. To this end, chlorobenzene/MeCN solutions of **2:Eu** ( $c = 164 \mu\text{mol L}^{-1}$ ) were drop-cast onto an ethylene vinyl alcohol copolymer and MSP coated polymer substrates were obtained by this process. Recorded fluorescence spectra of the coated substrates indicate the presence of a minor fraction of free ligand, which is assumed to arise due differences in the drying kinetics and renders the visual luminescence colour of the latter magenta (Fig. 4f and S20†). The **2:Eu** MSP-based coatings on such polymer supports were subsequently exposed to the different types of analytes and the emission was monitored visually and spectroscopically for detectable colour changes. Gratifyingly, the coatings displayed responses similar to those observed for thin MSP films on glass substrates when exposed to the different analytes. Thus, exposure to vapours emanating from DMSO, neat TEP, *n*-butylamine, or hydrochloric acid all furnished luminescence colour changes of the coated polymers (Fig. 4f and S20†).

## Conclusions

A  $\pi$ -extended Mebip ligand derivative was developed that displays a visually detectable blue fluorescence and allows for the reliable formation of metal-ion complexes analogous to the parent derivative. A telechelic macromonomer that carries this ligand was used to prepare thin polymer films and coatings of MSPs with  $\text{Eu}^{3+}$  ions. The latter display the characteristic red,  $\text{Eu}^{3+}$ -based luminescence colour and a visual luminescence colour change is obtained when external stimuli such as heat, solvents (liquid or vapour), or other analytes disrupt or alter the metal-ligand complexes. The developed metallosupramolecular materials can be readily processed into sensor devices that are, amongst others, potentially useful for the detection of harmful analytes such as CWAs.

## Conflicts of interest

There are no conflicts to declare.

## Acknowledgements

L. N., C. C., S. S., and C. W. gratefully acknowledge financial support through the National Center of Competence in Research Bio-Inspired Materials, a research instrument of the Swiss National Science Foundation as well as the Adolphe Merkle Foundation.

## References

- 1 D. Wu, A. C. Sedgwick, T. Gunnlaugsson, E. U. Akkaya, J. Yoon and T. D. James, *Chem. Soc. Rev.*, 2017, **46**, 7105–7123.
- 2 M. L. Aulsebrook, B. Graham, M. R. Grace and K. L. Tuck, *Coord. Chem. Rev.*, 2017, DOI: 10.1016/j.ccr.2017.11.018.
- 3 G. H. Dennison, C. G. Bochet, C. Curty, J. Ducry, D. J. Nielsen, M. R. Sambrook, A. Zaugg and M. R. Johnston, *Eur. J. Inorg. Chem.*, 2016, **2016**, 1348–1358.
- 4 M. Burnworth, S. J. Rowan and C. Weder, *Chem. – Eur. J.*, 2007, **13**, 7828–7836.
- 5 G. H. Dennison and M. R. Johnston, *Chem. – Eur. J.*, 2015, **21**, 6328–6338.
- 6 R. Shunmugam and G. N. Tew, *Chem. – Eur. J.*, 2008, **14**, 5409–5412.
- 7 D. Knapton, M. Burnworth, S. J. Rowan and C. Weder, *Angew. Chem., Int. Ed.*, 2006, **45**, 5825–5829.
- 8 C. Calvino, A. Guha, C. Weder and S. Schrettl, *Adv. Mater.*, 2018, **30**, 1704603.
- 9 S. E. Plush and T. Gunnlaugsson, *Dalton Trans.*, 2008, 3801–3804.
- 10 C. Song, Z. Ye, G. Wang, J. Yuan and Y. Guan, *Chem. – Eur. J.*, 2010, **16**, 6464–6472.
- 11 Y. Seto, in *Handbook of Toxicology of Chemical Warfare Agents*, ed. R. C. Gupta, Academic Press, Boston, 2 edn, 2015, ch. 60, pp. 897–914.
- 12 K. M. Herbert, S. Schrettl, S. J. Rowan and C. Weder, *Macromolecules*, 2017, **50**, 8845–8870.
- 13 A. J. Metherell, C. Curty, A. Zaugg, S. T. Saad, G. H. Dennison and M. D. Ward, *J. Mater. Chem. C*, 2016, **4**, 9664–9668.
- 14 S. Sarkar, A. Mondal, A. K. Tiwari and R. Shunmugam, *Chem. Commun.*, 2012, **48**, 4223–4225.
- 15 J. R. Kumpfer, J. Jin and S. J. Rowan, *J. Mater. Chem.*, 2010, **20**, 145–151.
- 16 P. Chen, Q. Li, S. Grindy and N. Holten-Andersen, *J. Am. Chem. Soc.*, 2015, **137**, 11590–11593.
- 17 A. Escande, L. Guénée, K.-L. Buchwalder and C. Piguet, *Inorg. Chem.*, 2009, **48**, 1132–1147.
- 18 K. Cheng and B. Tieke, *RSC Adv.*, 2014, **4**, 25079–25088.
- 19 P. K. Iyer, J. B. Beck, C. Weder and S. J. Rowan, *Chem. Commun.*, 2005, 319–321.
- 20 M. Burnworth, L. Tang, J. R. Kumpfer, A. J. Duncan, F. L. Beyer, G. L. Fiore, S. J. Rowan and C. Weder, *Nature*, 2011, **472**, 334–337.
- 21 J. C. Bunzli and C. Piguet, *Chem. Soc. Rev.*, 2005, **34**, 1048–1077.
- 22 D. W. Balkenende, S. Coulibaly, S. Balog, Y. C. Simon, G. L. Fiore and C. Weder, *J. Am. Chem. Soc.*, 2014, **136**, 10493–10498.
- 23 R. Diaz-Torres and S. Alvarez, *Dalton Trans.*, 2011, **40**, 10742–10750.

